ACS Macro Letters

Letter

pubs.acs.org/macroletters

# Janus-Dendrimer-Mediated Formation of Crystalline Virus Assemblies

Joona Mikkilä,[†] Henna Rosilo,[†] Sami Nummelin,[†] Jani Seitsonen,[†] Janne Ruokolainen,[†] and Mauri A. Kostiainen*[,†,‡]

[†]Molecular Materials, Department of Applied Physics, Aalto University, 00076 Espoo, Finland

[‡]Biohybrid Materials, Department of Biotechnology and Chemical Technology, Aalto University, 00076 Espoo, Finland

Supporting Information

**ABSTRACT:** Amphiphilic dendrimers have been shown to self-assemble with nanosized protein particles (viruses) to form highly ordered hierarchical assemblies. Here we present Janus-type dendrimers that have been synthesized from Newkome-type dendrons with hydrophilic spermine groups and hydrophobic Percec-type dendrons. These amphiphilic dendrimers bind electrostatically on the surface of virus particles and co-assemble into crystalline complexes with a lattice constant ($a$ = 42 nm) comparable to the size of the virus particles. Small-angle X-ray scattering and cryogenic transmission electron microscopy show that the complexes have a face-centered cubic structure (space group $Fm\bar{3}m$) and remarkable long-range order. Results indicate that amphiphilic dendrimers can be utilized to create inclusion body mimicking nanostructures.

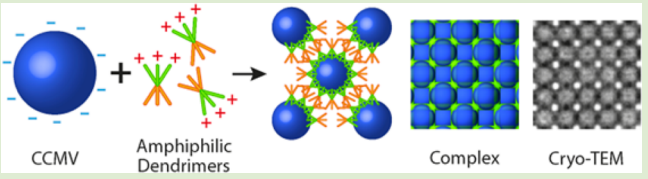


Inclusion bodies are intracellular protein or virus complexes that often exhibit crystalline order. They have been found in biological systems ranging from algae to the human brain[1−3] and observed to play a central role in many complex biological events and diseases. For example, Ebola virus inclusion bodies are the site of viral RNA replication.[4] In the case of Huntington's disease, inclusion body formation is a beneficial coping response to the death of selected neuron types,[3,5] suggesting that such systems could facilitate the development of effective treatments. Due to the complex nature of inclusion bodies, their mechanism of formation and hierarchical structure is unclear in many cases. Thus, the design and fabrication of model systems would facilitate their research. Herein, we have studied the self-assembly and structural control of viral inclusion body mimicking nanostructures and demonstrate that crystalline structures can be assembled using amphiphilic Janus-dendrimers and native Cowpea Chlorotic Mottle Virus (CCMV) particles.[6]

Previous research on nanostructures that structurally resemble inclusion bodies has utilized different proteins,[7−9] viruses,[10−13] or DNA[13,14] that self-assemble with peptides,[7] lipids,[13,14] or polymers[12] to form amorphous or hierarchical complexes. For example, small tetragonal 2D arrays have been prepared from histidine-tagged proteins and gold nanoparticles (AuNPs) interconnecting the tag sites.[15] An extension to 3D structures was achieved by using DNA-mediated assembly of AuNPs and Q$\beta$ capsid nanoparticles to create crystalline complexes with a NaTl lattice.[16] Programmable atom mimicry[17] has also been reached when utilizing DNA-coated metal nanoparticles to assemble into 3D colloidal crystals.[18] Our preceding studies show that virus and ferritin particles form crystalline complexes with gold nanoparticles[19] and cationic polymers,[20,21] especially with dendrimers and dendrons.[21,22]

Dendrimers and dendrons are periodically branched macromolecules with several remarkable properties, such as well-defined, monodisperse structure and the ability to encapsulate functional materials. They are capable of binding biomolecules with multivalent interactions and can function as supramolecular glue or building blocks for hierarchical assemblies.[23−30] Amphiphilic Janus-dendrimers expand the scope by combining two distinct chemical functionalities in a single molecule and thus can function as powerful structure-directing tectons[31−33] for biomolecular complexes with greater versatility than regular dendrimers.[14,34−37]

In this work, four new amphiphilic dendrimers were synthesized (Figure 1) by combining hydrophobic Percec-type dendrons[38,39] with spermine-modified Newkome-type dendrons.[40] Amine groups (p$K_a$ > 8) at the hydrophilic spermine tails are positively charged under the experimental conditions, which enables electrostatic binding to the negatively charged (pI = 3.8) surface of CCMV. The virus consists of RNA encapsulated by 180 identical coat protein subunits,[41] which form an icosahedral capsid with a diameter of 28 nm. The multivalent structure of the Janus-dendrimers **2C$_{12}$-G1**, **3C$_{12}$-G0**, **3C$_{12}$-G1**, and **6C$_{12}$-G1** enables high-affinity electrostatic binding of CCMV, which is further enhanced by their amphiphilic nature.[35,42]

We investigated the co-assembly of dendrimers and virus particles and were able to develop a structure−activity

**Received:** June 13, 2013
**Accepted:** July 22, 2013
**Published:** July 24, 2013

   dx.doi.org/10.1021/mz400307h | *ACS Macro Lett.* 2013, 2, 720−724

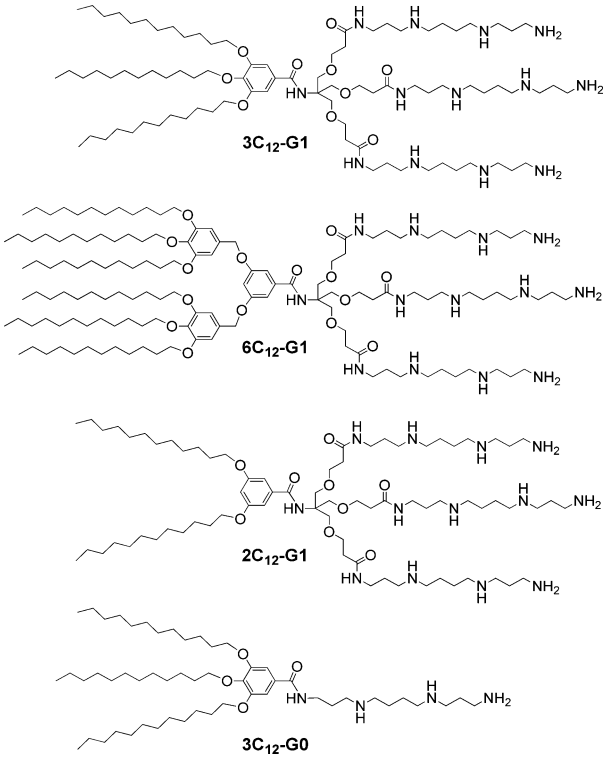


**Figure 1.** Amphiphilic spermine-alkyl dendrimers applied to bind virus particles.

relationship between the dendrimer structure, CCMV binding efficiency, and the nanostructure of the co-assembled complex. This approach can be applied in future investigations of inclusion body mimicking nanostructures and can have wider implications in the preparation of functional metamaterials, due to CCMV's ability to encapsulate various nanoparticles.[6,43]

The ability of the dendrimers to form complexes with CCMV was examined by gel electrophoresis and dynamic light scattering (DLS). In DLS measurements a CCMV solution (60 mg $L^{-1}$) was titrated by adding small volumes of dendrimer solution in the presence of 0 or 150 mM NaCl. In the absence of dendrimer only the peak (27.3 nm) resulting from the free CCMV can be observed in the size-distribution profile (Figure 2a). When the **$3C_{12}$-G1** dendrimer is added incrementally to the CCMV solution, the peak of free CCMV decreased, and another peak corresponding to large CCMV−dendrimer complexes appeared. Above 4 mg $L^{-1}$ dendrimer concentrations, free CCMV was not detected anymore. The size of the secondary assemblies increased with the dendrimer concentration until micrometer-sized assemblies were formed. Figure 2b,c presents how the intensity of free CCMV decreased, whereas the size of the secondary assembly increased when a CCMV solution was titrated with **$3C_{12}$-G1** dendrimer in 0 and 150 mM NaCl solutions, respectively. The titration results for **$6C_{12}$-G1**, **$2C_{12}$-G1**, and **$3C_{12}$-G0** are presented in the Supporting Information (Figure S1).

The effect of NaCl on the size of the complexes and formation efficiency was clearly observed. In both NaCl concentrations the CCMV binding efficiency of different dendrimers decreased in the following order: **$3C_{12}$-G1** > **$6C_{12}$-G1** > **$2C_{12}$-G1** > **$3C_{12}$-G0**. The binding efficiencies of different dendrimers can be described with a $c_{20}$ value, which defines the dendrimer concentrations needed to lower the intensity of free CCMV to 20% of the original (Table 1).

**Table 1. Dendrimer Concentrations Needed to Decrease the Intensity of Free CCMV to 20% as Observed by DLS Measurements ($c_{20}$ Values)**

| Janus-dendrimer | $c_{20}$ (mg $L^{-1}$) 0 mM NaCl | $c_{20}$ (mg $L^{-1}$) 150 mM NaCl |
|---|---|---|
| **$3C_{12}$-G1** | 1.9 | 1.0 |
| **$6C_{12}$-G1** | 3.5 | 2.6 |
| **$2C_{12}$-G1** | 4.3 | 5.5 |
| **$3C_{12}$-G0** | 11.2 | 21.3 |

Interestingly, the **$3C_{12}$-G1** and **$6C_{12}$-G1** complexed CCMV more effectively in 150 mM ($c_{20}$ values 1.0 and 2.6, respectively) than in 0 mM NaCl ($c_{20}$ 1.9 and 3.5) solution, even though electrostatic interactions are weaker in higher ionic strength. At the same time **$2C_{12}$-G1** and **$3C_{12}$-G0** had lower binding efficiencies in the 150 mM NaCl ($c_{20}$ 5.5 and 21.3) than in the 0 mM NaCl ($c_{20}$ 4.3 and 11.2) concentration. This observation can be attributed to the fact that increasing the electrolyte concentration decreases the solubility of the nonpolar parts of the amphiphilic dendrimers, which may drive the dendrimers to form higher-order structures and to further enhance the complex formation.

Because **$3C_{12}$-G1** and **$6C_{12}$-G1** have larger nonpolar volume fractions than **$2C_{12}$-G1**, increasing the salt concentration results in stronger binding due to self-assembled multivalency.[44] In the case of **$3C_{12}$-G0**, having only one spermine group, the higher salt concentration screens the electrostatic binding more efficiently than in the case of **$2C_{12}$-G1**, **$3C_{12}$-G1**, and **$6C_{12}$-G1** dendrimers. This leads to significantly lower binding efficiency in 150 mM NaCl solution than in 0 mM NaCl solution. Also, the maximum secondary assembly sizes were

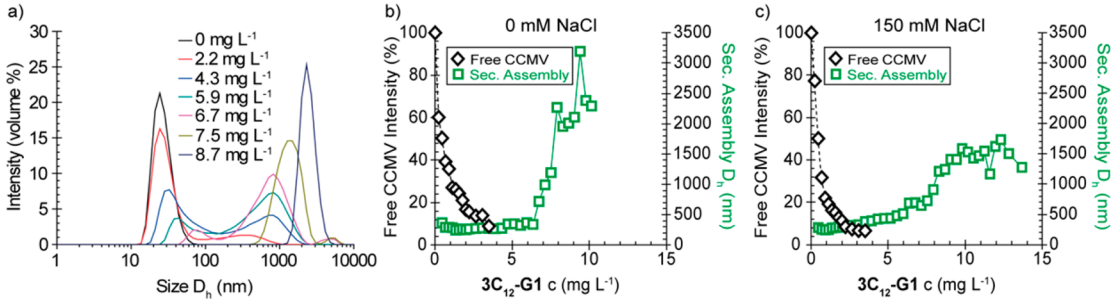


**Figure 2.** (a) DLS results showing the change in the volume-averaged size distribution profile when CCMV solution is titrated with **$3C_{12}$-G1** in the absence of NaCl. (b, c) DLS results presenting the changes in free CCMV scattering intensity and secondary assembly size, when CCMV solution is titrated with **$3C_{12}$-G1** in (b) 0 mM NaCl and (c) 150 mM NaCl solutions.


dx.doi.org/10.1021/mz400307h | *ACS Macro Lett.* 2013, 2, 720−724

smaller in 150 mM salt concentration (1000−2500 nm) than in the absence of added electrolyte (2000−3500 nm). This behavior was observed with all dendrimers except **3C$_{12}$-G0**, which had significantly smaller secondary assembly size in both NaCl concentrations. Overall, the **3C$_{12}$-G1** dendrimer is the most efficient CCMV binder due to its ideal balance between hydrophobicity and the number of spermine units.

The morphology of CCMV−dendrimer complexes was studied by small-angle X-ray scattering (SAXS) and cryogenic transmission electron microscopy (cryo-TEM). SAXS results for CCMV−dendrimer complexes formed in nine different NaCl concentrations (0−300 mM range) are presented in the Supporting Information (Figures S3−S6). Different NaCl concentrations were investigated to tune the dendrimer−CCMV interaction as well as the crystallinity of the resulting inclusion body mimicking structure (Figure S7, Supporting Information). For example, CCMV−**3C$_{12}$-G1** complexes formed in the absence of NaCl or below 120 mM NaCl concentrations exhibited an amorphous structure as indicated by the broad SAXS reflections and the cryo-TEM image (Figure 3a). However, when the ionic strength was further increased to 160−250 mM, self-assembled crystalline structures were identified (Figure 3b). Also, cryo-TEM images obtained from 250 to 300 mM NaCl samples clearly show highly crystalline virus arrays (Figure 3c, see the Supporting Information Figure S8 for a magnification). When the NaCl concentration was increased even further to 625 mM, the electrostatic interaction between viruses and dendrimers was lost, and no complexes could be found (Figure 3d). In SAXS measurements all scattering peaks from CCMV−dendrimer complexes showed the smallest full width at half-maximum values (fwhm) at 160−250 mM NaCl solutions, indicating that the crystal domains are more pronounced in these electrolyte concentrations. The most efficient crystal formation was therefore observed on the onset of electrolyte-induced disassembly, where the electrostatic interactions are weak enough to avoid kinetically trapped structures. Differing from other Janus-dendrimers, **3C$_{12}$-G0** and **6C$_{12}$-G1** form complexes with much smaller crystal domain size in the studied electrolyte concentrations, which can be observed as broad SAXS reflections.

Figure 3e presents an experimental SAXS curve measured from the CCMV−**3C$_{12}$-G1** complex and a comparison to calculated finite face-centered cubic (fcc) and perfect calcium fluoride ($CaF_2$) structures. The experimental data can be reliably fitted with an fcc (space group $Fm\bar{3}m$) Bravais lattice. In the measured curve, SAXS reflections at $q$ = 0.26, 0.44, 0.51, and 0.69 nm$^{-1}$ were clearly observed, which correspond to the SAXS reflections from the ($hkl$) = (111), (220), (311), (331)/(420) planes, respectively. Ratios of the observed SAXS reflections divided by $q^*$ (0.15 nm) ($q^n/q^*$) are then approximately $\sqrt{3}:\sqrt{8}:\sqrt{11}:\sqrt{19}$, indicating an fcc structure (Figure 3e). The lattice parameter ($a = 2\pi/q^*$) of the structure is 41.6 nm, and the calculated distance between virus particle centers ($d = a/\sqrt{2}$) is 29.4 nm, which corresponds well to the CCMV diameter (28 nm). Furthermore, the measured data do not show clear reflections from the (200), (222), and (420) planes, suggesting that the tetrahedral voids between the CCMV particles are occupied. We therefore argue that the dendrimers can form micellar structures that are primarily located in the tetrahedral voids to yield a lattice that is isostructural with $CaF_2$ (Figure 4a).

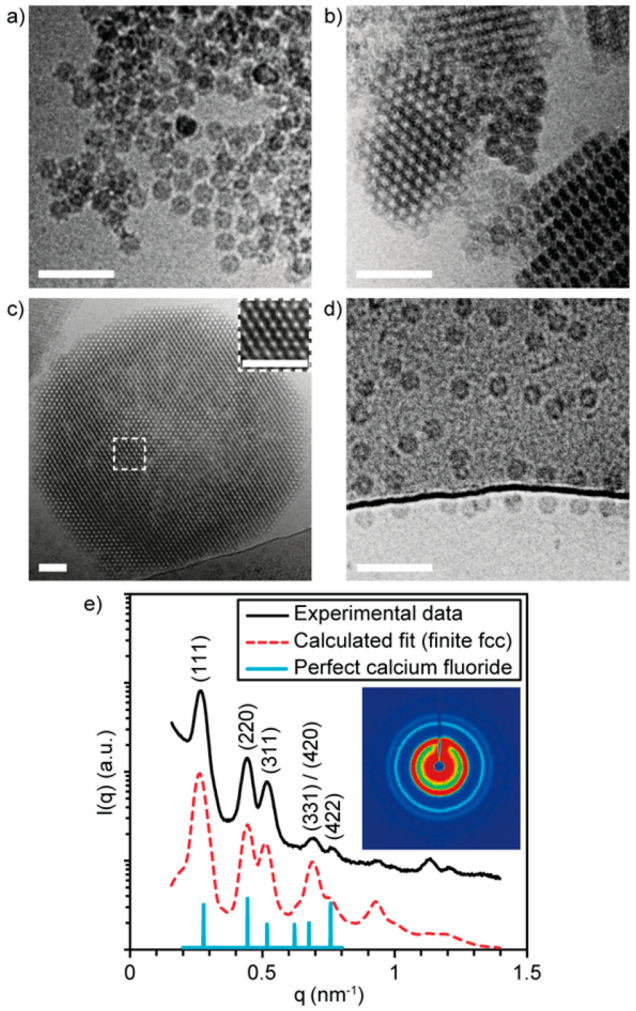


**Figure 3.** Cryo-TEM images of CCMV mixed with **3C$_{12}$-G1** dendrimer in (a) 0 mM, (b) 250 mM, (c) 300 mM, and (d) 625 mM NaCl solutions. Scale bar is 100 nm. (e) Integrated SAXS data measured from the CCMV−**3C$_{12}$-G1** complex in 250 mM NaCl concentration and its comparison to calculated scattering curves from finite *fcc* and perfect calcium fluoride structures. Inset: 2D scattering pattern.

Cryo-TEM images (Figures 4b, c, and d) confirm that the **3C$_{12}$-G1** dendrimers fill the tetrahedral voids and may also partially form tubular structures that connect the tetrahedral voids. Earlier studies on co-assembly and tubular structures self-assembled from dendritic molecules are in agreement with our results.[25,26,32,45] The images present the expected CCMV-dendrimer crystal projections viewed along the [100], [110], and [111] zone axes, respectively. The lattice constant $a$ determined from these images is 41.9 nm. Overall, the cryo-TEM images are in excellent agreement with the crystallographic arrangement and the lattice parameter obtained from the SAXS results.

In conclusion, we have shown that Janus-dendrimers and CCMV virus particles can self-assemble into complexes that structurally mimic viral inclusion bodies. Furthermore, our results can be utilized when defining the principles of nanoscale atom mimicry.[17] We suggest that to achieve the best binding efficiency and optimized crystal formation with the dendrimers presented here the number of spermine and alkyl chains should be approximately the same. Furthermore, the dendrimer should


dx.doi.org/10.1021/mz400307h | *ACS Macro Lett.* 2013, 2, 720−724

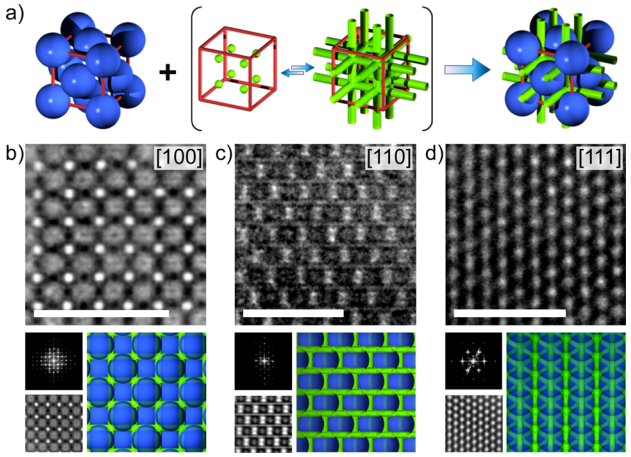


**Figure 4.** (a) Co-assembly of CCMV particles (blue) and Janus-dendrimers (green). (b–d) Images divided into groups according to view along different zone axes [100] (b), [110] (c), and [111] (d). Groups consist of the cryo-TEM image of the CCMV–$3C_{12}$-**G1** superlattice formed in 250 or 300 mM NaCl solutions (top, scale bar 100 nm), Fourier transform (middle left), filtered inverse Fourier transform (bottom left), and a schematic illustration (bottom right).

have more than one spermine ligand to achieve multivalent binding. This is because $3C_{12}$-**G0** fails to bind CCMV efficiently under physiological conditions, and $6C_{12}$-**G1** does not bind CCMV as effectively as $3C_{12}$-**G1** even though it has a larger hydrophobic part. In addition, smaller crystal domain sizes were observed in the SAXS measurements for the CCMV–$6C_{12}$-**G1** complex compared to those formed with $3C_{12}$-**G1**. To obtain crystalline virus arrays, careful tuning of the electrostatic interactions to the onset of electrolyte-induced disassembly is required. The results presented here can be applied when creating model inclusion bodies and may find applications in studying complex biological systems. Furthermore, this approach can be utilized when creating new biohybrid metamaterials via self-assembly.

## ■ ASSOCIATED CONTENT

### Ⓢ Supporting Information

Experimental details and additional data. This material is available free of charge via the Internet at http://pubs.acs.org.

## ■ AUTHOR INFORMATION

### Corresponding Author

*E-mail: mauri.kostiainen@aalto.fi.

### Notes

The authors declare no competing financial interest.

## ■ ACKNOWLEDGMENTS

This work was supported by the Emil Aaltonen Foundation (J.M.) and the Academy of Finland (grant No. 138850 for S.N. and 137582 for M.A.K.). We acknowledge Panu Hiekkataipale for fruitful discussion and SAXS support.

## ■ REFERENCES

(1) Suttle, C. A. *Nature* **2005**, *437*, 356–361.
(2) Lowe, J.; Blanchard, A.; Morrell, K.; Lennox, G.; Reynolds, L.; Billett, M.; Landon, M.; Mayer, R. J. *J. Pathol.* **1988**, *155*, 9–15.
(3) Arrasate, M.; Mitra, S.; Schweitzer, E. S.; Segal, M. R.; Finkbeiner, S. *Nature* **2004**, *431*, 805–810.
(4) Hoenen, T.; Shabman, R. S.; Groseth, A.; Herwig, A.; Weber, M.; Schudt, G.; Dolnik, O.; Basler, C. F.; Becker, S.; Feldmann, H. *J. Virol.* **2012**, *86*, 11779–11788.
(5) Miller, J.; Arrasate, M.; Shaby, B. A.; Mitra, S.; Masliah, E.; Finkbeiner, S. *J. Neurosci.* **2010**, *30*, 10541–10550.
(6) Uchida, M.; Klem, M. T.; Allen, M.; Suci, P.; Flenniken, M.; Gillitzer, E.; Varpness, Z.; Liepold, L. O.; Young, M.; Douglas, T. *Adv. Mater.* **2007**, *19*, 1025–1042.
(7) Zhou, B.; Xing, L.; Wu, W.; Zhang, X.-E.; Lin, Z. *Microb. Cell Fact.* **2012**, *11*, 10.
(8) Brodin, J. D.; Ambroggio, X. I.; Tang, C.; Parent, K. N.; Baker, T. S.; Tezcan, F. A. *Nat. Chem.* **2012**, *4*, 375–382.
(9) Sinclair, J. C.; Davies, K. M.; Vénien-Bryan, C.; Noble, M. E. M. *Nat. Nanotechnol.* **2011**, *6*, 558–562.
(10) Nedoluzhko, A.; Douglas, T. *J. Inorg. Biochem.* **2001**, *84*, 233–240.
(11) Oh, D.; Dang, X.; Yi, H.; Allen, M. A.; Xu, K.; Lee, Y. J.; Belcher, A. M. *Small* **2012**, *8*, 1006–1011.
(12) Cheung, C. L.; Rubinstein, A. I.; Peterson, E. J.; Chatterji, A.; Sabirianov, R. F.; Mei, W.-N.; Lin, T.; Johnson, J. E.; DeYoreo, J. J. *Langmuir* **2010**, *26*, 3498–3505.
(13) Yang, L.; Liang, H.; Angelini, T. E.; Butler, J.; Coridan, R.; Tang, J. X.; Wong, G. C. L. *Nat. Mater.* **2004**, *3*, 615–619.
(14) Ewert, K. K.; Evans, H. M.; Zidovska, A.; Bouxsein, N. F.; Ahmad, A.; Safinya, C. R. *J. Am. Chem. Soc.* **2006**, *128*, 3998–4006.
(15) Hu, M.; Qian, L.; Briñas, R. P.; Lymar, E. S.; Hainfeld, J. F. *Angew. Chem., Int. Ed.* **2007**, *46*, 5111–5114.
(16) Cigler, P.; Lytton-Jean, A. K. R.; Anderson, D. G.; Finn, M. G.; Park, S. Y. *Nat. Mater.* **2010**, *9*, 918–922.
(17) Tomalia, D. A. *J. Nanopart. Res.* **2009**, *11*, 1251–1310.
(18) Zhang, C.; Macfarlane, R. J.; Young, K. L.; Choi, C. H. J.; Hao, L.; Auyeung, E.; Liu, G.; Zhou, X.; Mirkin, C. A. *Nat. Mater.* **2013**, DOI: 10.1038/nmat3647.
(19) Kostiainen, M. A.; Hiekkataipale, P.; Laiho, A.; Lemieux, V.; Seitsonen, J.; Ruokolainen, J.; Ceci, P. *Nat. Nanotechnol.* **2013**, *8*, 52–56.
(20) Kostiainen, M. A.; Pietsch, C.; Hoogenboom, R.; Nolte, R. J. M.; Cornelissen, J. J. L. M. *Adv. Funct. Mater.* **2011**, *21*, 2012–2019.
(21) Kostiainen, M. A.; Hiekkataipale, P.; de la Torre, J. Á.; Nolte, R. J. M.; Cornelissen, J. J. L. M. *J. Mater. Chem.* **2011**, *21*, 2112–2117.
(22) Kostiainen, M. A.; Kasyutich, O.; Cornelissen, J. J. L. M.; Nolte, R. J. M. *Nat. Chem.* **2010**, *2*, 394–399.
(23) Balagurusamy, V. S. K.; Ungar, G.; Percec, V.; Johansson, G. *J. Am. Chem. Soc.* **1997**, *119*, 1539–1555.
(24) Yeardley, D. J. P.; Ungar, G.; Percec, V.; Holerca, M. N.; Jahansson, G. *J. Am. Chem. Soc.* **2000**, *122*, 1684–1689.
(25) Hudson, S. D.; Jung, H.-T.; Percec, V.; Cho, W.-D.; Johansson, G.; Ungar, G.; Balagurusamy, V. S. K. *Science* **1997**, *278*, 449–452.
(26) Ungar, G.; Liu, Y.; Zeng, X.; Percec, V.; Cho, W.-D. *Science* **2003**, *299*, 1208–1211.
(27) Esfand, R.; Tomalia, D. A. *Drug Discovery Today* **2001**, *6*, 427–436.
(28) Tomalia, D. A. *Soft Matter* **2010**, *6*, 456–474.
(29) Tomalia, D. A.; Brothers, H. M.; Piehler, L. T.; Durst, H. D.; Swanson, D. R. *Proc. Natl. Acad. Sci. U.S.A.* **2002**, *99*, 5081–5087.
(30) Peterca, M.; Percec, V.; Leowanawat, P.; Bertin, A. *J. Am. Chem. Soc.* **2011**, *133*, 20507–20520.
(31) Percec, V.; Peterca, M.; Dulcey, A. E.; Imam, M. R.; Hudson, S. D.; Nummelin, S.; Adelman, P.; Heiney, P. A. *J. Am. Chem. Soc.* **2008**, *130*, 13079–13094.
(32) Percec, V.; Wilson, D. A.; Leowanawat, P.; Wilson, C. J.; Hughes, A. D.; Kaucher, M. S.; Hammer, D. A.; Levine, D. H.; Kim, A. J.; Bates, F. S.; Davis, K. P.; Lodge, T. P.; Klein, M. L.; DeVane, R. H.; Aqad, E.; Rosen, B. M.; Argintaru, A. O.; Sienkowska, M. J.; Rissanen, K.; Nummelin, S.; Ropponen, J. *Science* **2010**, *328*, 1009–1014.
(33) Percec, V.; Leowanawat, P.; Sun, H.-J.; Kulikov, O.; Nusbaum, C. D.; Tran, T. M.; Bertin, A.; Wilson, D. A.; Peterca, M.; Zhang, S.; Kamat, N. P.; Vargo, K.; Moock, D.; Johnston, E. D.; Hammer, D. A.; Pochan, D. J.; Chen, Y.; Chabre, Y. M.; Shiao, T. C.; Bergeron-Brlek,

M.; André, S.; Roy, R.; Gabius, H.-J.; Heiney, P. A. *J. Am. Chem. Soc.* **2013**, *135*, 9055−9077.
(34) Joester, D.; Losson, M.; Pugin, R.; Heinzelmann, H.; Walter, E.; Merkle, H. P.; Diederich, F. *Angew. Chem., Int. Ed.* **2003**, *42*, 1486−1490.
(35) Röglin, L.; Lempens, E. H. M.; Meijer, E. W. *Angew. Chem., Int. Ed.* **2011**, *50*, 102−112.
(36) Barnard, A.; Posocco, P.; Pricl, S.; Calderon, M.; Haag, R.; Hwang, M. E.; Shum, V. W. T.; Pack, D. W.; Smith, D. K. *J. Am. Chem. Soc.* **2011**, *133*, 20288−20300.
(37) Shiao, T. C.; Roy, R. *New J. Chem.* **2012**, *36*, 324−339.
(38) Rosen, B. M.; Wilson, C. J.; Wilson, D. A.; Peterca, M.; Imam, M. R.; Percec, V. *Chem. Rev.* **2009**, *109*, 6275−6540.
(39) Percec, V.; Cho, W.; Ungar, G.; Yeardley, D. *Angew. Chem., Int. Ed.* **2000**, *39*, 1597−1602.
(40) Kostiainen, M. A.; Hardy, J. G.; Smith, D. K. *Angew. Chem., Int. Ed.* **2005**, *44*, 2556−2559.
(41) Speir, J. A.; Munshi, S.; Wang, G.; Baker, T. S.; Johnson, J. E. *Structure* **1995**, *3*, 63−78.
(42) Mammen, M.; Choi, S.-K.; Whitesides, G. M. *Angew. Chem., Int. Ed.* **1998**, *37*, 2754−2794.
(43) Douglas, T.; Young, M. *Nature* **1998**, *393*, 152−155.
(44) Barnard, A.; Smith, D. K. *Angew. Chem., Int. Ed.* **2012**, *51*, 6572−6581.
(45) Percec, V.; Glodde, M.; Bera, T. K.; Miura, Y.; Shiyanovskaya, I.; Singer, K. D.; Balagurusamy, V. S. K.; Heiney, P. A.; Schnell, I.; Rapp, A.; Spiess, H.-W.; Hudson, S. D.; Duan, H. *Nature* **2002**, *419*, 384−387.